Stem Cell Reports
Report
ISSCR
OPEN ACCESS

Channelopathy as a SUDEP Biomarker in Dravet Syndrome Patient-Derived Cardiac Myocytes

Chad R. Frasier,[1,9] Helen Zhang,[2,9] James Offord,[1] Louis T. Dang,[3] David S. Auerbach,[1,8] Huilin Shi,[2] Chunling Chen,[1] Alica M. Goldman,[4,5] L. Lee Eckhardt,[6] Vassilios J. Bezzerides,[7] Jack M. Parent,[2,4,10,*] and Lori L. Isom[1,2,10,*]

[1]Department of Pharmacology, University of Michigan Medical School, 2301E MSRB III, Ann Arbor, MI 48109, USA
[2]Department of Neurology, University of Michigan Medical School, 5021 BSRB, Ann Arbor, MI 48109, USA
[3]Division of Pediatric Neurology, Department of Pediatrics and Communicable Diseases, University of Michigan Medical School, Ann Arbor, MI 48109, USA
[4]Ann Arbor VA Healthcare System, University of Michigan Medical School, Ann Arbor, MI 48109, USA
[5]Department of Neurology, Baylor College of Medicine, Houston, TX 77030, USA
[6]Cellular and Molecular Arrhythmia Research Program, Division of Cardiovascular Medicine, University of Wisconsin, Madison, WI 53705, USA
[7]Cardiology, Electrophysiology Division, Boston Children's Hospital, Boston, MA 02115, USA
[8]Present address: Department of Pharmacology and Physiology, University of Rochester School of Medicine and Dentistry, Rochester, NY 14642, USA
[9]Co-first author
[10]Co-senior author
*Correspondence: parent@umich.edu (J.M.P.), lisom@umich.edu (L.L.I.)
https://doi.org/10.1016/j.stemcr.2018.07.012

SUMMARY

Dravet syndrome (DS) is a severe developmental and epileptic encephalopathy with a high incidence of sudden unexpected death in epilepsy (SUDEP). Most DS patients carry *de novo* variants in *SCN1A*, resulting in $Na_v1.1$ haploinsufficiency. Because *SCN1A* is expressed in heart and in brain, we proposed that cardiac arrhythmia contributes to SUDEP in DS. We generated DS patient and control induced pluripotent stem cell-derived cardiac myocytes (iPSC-CMs). We observed increased sodium current (I_{Na}) and spontaneous contraction rates in DS patient iPSC-CMs versus controls. For the subject with the largest increase in I_{Na}, cardiac abnormalities were revealed upon clinical evaluation. Generation of a CRISPR gene-edited heterozygous *SCN1A* deletion in control iPSCs increased I_{Na} density in iPSC-CMs similar to that seen in patient cells. Thus, the high risk of SUDEP in DS may result from a predisposition to cardiac arrhythmias in addition to seizures, reflecting expression of *SCN1A* in heart and brain.

INTRODUCTION

Dravet syndrome (DS) is a severe and intractable developmental and epileptic encephalopathy characterized by pharmacoresistant seizures, cognitive impairment, and increased mortality. The majority of DS patients carry *de novo* variants in *SCN1A* that result in haploinsufficiency for the voltage-gated sodium channel (VGSC) $Na_v1.1$ (Claes et al., 2001; Meisler and Kearney, 2005). Up to 20% of DS patients die from sudden unexpected death in epilepsy (SUDEP) (Cooper et al., 2016). Indirect evidence has linked SUDEP to central or obstructive apnea, pulmonary edema, dysregulation of cerebral circulation, autonomic dysfunction, or cardiac arrhythmias (Surges et al., 2009). While SUDEP is the most devastating consequence of epilepsy, very little is understood about its causes and there are no biomarkers to predict which patients are at increased risk for SUDEP. Because *SCN1A* is expressed in heart as well as in brain (Malhotra et al., 2001; Mishra et al., 2015), we proposed that alterations in cardiac excitability may contribute to the mechanism of SUDEP in *SCN1A*-linked DS. Here, we used DS patient induced pluripotent stem cell-derived cardiac myocytes (iPSC-CMs) to test this hypothesis.

The cardiac action potential (AP) is a tightly regulated process that relies on the ability of ion channels to depolarize and repolarize in synchrony to maintain proper heart rhythm (Roden et al., 2002). Mutations in cardiac VGSC genes result in arrhythmias (Veerman et al., 2015). Tetrodotoxin (TTX)-resistant $Na_v1.5$ channels, encoded by *SCN5A*, are the major cardiac VGSCs in mammals (Bao and Isom, 2014). $Na_v1.1$, a TTX-sensitive VGSC that is highly expressed in brain (Westenbroek et al., 1989), is also expressed in human and mouse heart, although at lower levels than $Na_v1.5$ (Malhotra et al., 2001; Mishra et al., 2015). Work in rodents indicates that TTX-sensitive VGSCs, including $Na_v1.1$, are expressed in specific cardiac subcellular domains where they play important roles in shaping the cardiac AP and modulating excitation-contraction coupling (Frasier et al., 2016; Lin et al., 2015; Maier et al., 2002, 2004; Radwanski et al., 2015; Westenbroek et al., 2013). We showed previously that *Scn1a*^{R1407X} and *Scn1b* null DS mouse CMs have compensatory increases in transient and persistent sodium current (I_{Na}) and increased incidence of early afterdepolarizations in the AP waveform (Auerbach et al., 2013; Lin et al., 2015; Lopez-Santiago et al., 2007). This work demonstrated that, in addition to aberrant central and peripheral neuronal excitability (Kalume et al., 2013; Yu et al., 2006), DS mice have differences in CM ionic currents that serve as substrates for arrhythmias. Importantly, our work suggested that

Table 1. Clinical Characterization of DS Patients

	DS2	DS4	DS5	DS10
Sex	**M**	**M**	**F**	**F**
SCN1A mutation	c.975T>A (p.Y325X)	c.3982T>C (p.S1328P)	c.664C>T (p.R222X)	c.G965>T (p.R322I)
Sample type	fibroblasts	fibroblasts	fibroblasts	fibroblasts
Age at skin biopsy (years)	7	7	2	10
Notes			cardiac evaluation at age 4 years showed abnormal T-wave inversions and lateral T-wave flattening	after this study, was diagnosed with Wolff-Parkinson-White syndrome and underwent successful ablation

cardiac arrhythmias contribute to the mechanism of SUDEP in DS patients.

While transgenic mouse models have provided valuable insights into potential SUDEP mechanisms, mice are not small humans. As a result, no biomarkers exist to assess SUDEP risk in patients. To address this problem, we have generated CMs from *SCN1A*-DS patient-derived iPSCs. Importantly, iPSC-CMs retain the patient's unique genetic background. In addition, cellular phenotypes are autonomous; changes in ionic currents are intrinsic to the cell rather than the result of remodeling in response to altered autonomic innervation or seizures, as might occur in the whole animal. Here, we generated iPSC-CMs from 4 *SCN1A*-linked DS subjects and two controls without epilepsy and measured contraction rates and VGSC function. Our results were predictive of altered cardiac electrophysiology in one subject before cardiac symptoms were diagnosed.

RESULTS

Skin biopsies were collected from four *SCN1A*-linked DS patients and two controls without epilepsy under Institutional Review Board approval. Table 1 characterizes the patient *SCN1A* mutations as well as their clinical parameters. Reprogramming and pluripotency analyses were described previously (Liu et al., 2013). To generate iPSC-CMs we used chemically defined, growth factor-free media containing small-molecule Wnt inhibitors (Lian et al., 2012). Following at least 60 days of maturation, iPSC-CMs had an elongated morphology (Figures 1A–1C and 2B). Immunofluorescence staining (Figures 1 and S1) showed that both patient and control iPSC-CMs expressed α-actinin (Figures 1A–1C and S1A–S1E), connexin 43 (Figures 1A and S1A–S1E), Nav1.5 (Figures 1B and S1A–S1E), and the homeobox transcription factor NKX2.5 (Figures 1C and S1A–S1E).

iPSC-CMs spontaneously contract in monolayer culture (Zhang et al., 2009). Video recordings of the contracting monolayers showed a higher rate of contraction for DS patient iPSC-CMs compared with controls, with no differences between DS patient lines (Figures 1D and S2; Video S1). We used multi-electrode array (MEA) recordings as an independent approach to assess contraction rates. Two lines, control 3 and DS4, were tested using this method. In agreement with visually quantified rate differences, the firing rate in the MEA recordings was increased in DS4 compared with control (Figures 1E, 1F, and S2C).

We performed whole-cell voltage-clamp recordings to investigate whether iPSC-CMs from DS patients had altered I_{Na} density due to compensatory expression of other VGSC genes, as observed in DS mouse models (Auerbach et al., 2013; Lopez-Santiago et al., 2007). Transient I_{Na} density was increased at least 1.5-fold in all four DS iPSC-CM lines (1.57-fold for DS2, 1.80-fold for DS4, 1.74-fold for DS10, and 2.37-fold for DS5) over control lines (Figures 2A and 2C–2E; Table S1). Current density in the DS5 CMs was so large that proper voltage control could not be consistently maintained and voltage-dependent properties could not be accurately measured (Figure 2E, inset; Table S1), thus the value reported for I_{Na} density is likely an underestimate of the true increase. The increase in DS5 I_{Na} density was significantly greater than the average increase observed in the other three DS patient lines ($p = 0.03$; Figure 2D and Table S1). We found no changes in persistent I_{Na} density between control and DS lines. DS10 showed a small but significant decrease in τ for the fast component of inactivation at −30 mV, with no changes in τ for the slow phase of inactivation between control and DS lines. DS4 and DS10 showed small but significant positive shifts in the voltage dependence of inactivation, with DS4 also showing a reduced slope of the inactivation curve compared with control. DS2 and DS10 showed negative shifts in the voltage dependence of activation as well as decreases in activation slope compared with control (Table S1).

We performed qRT-PCR (Figure 2F) to assess changes in the level of VGSC mRNA expression in DS patient iPSC-CMs compared with control iPSC-CMs and non-failing

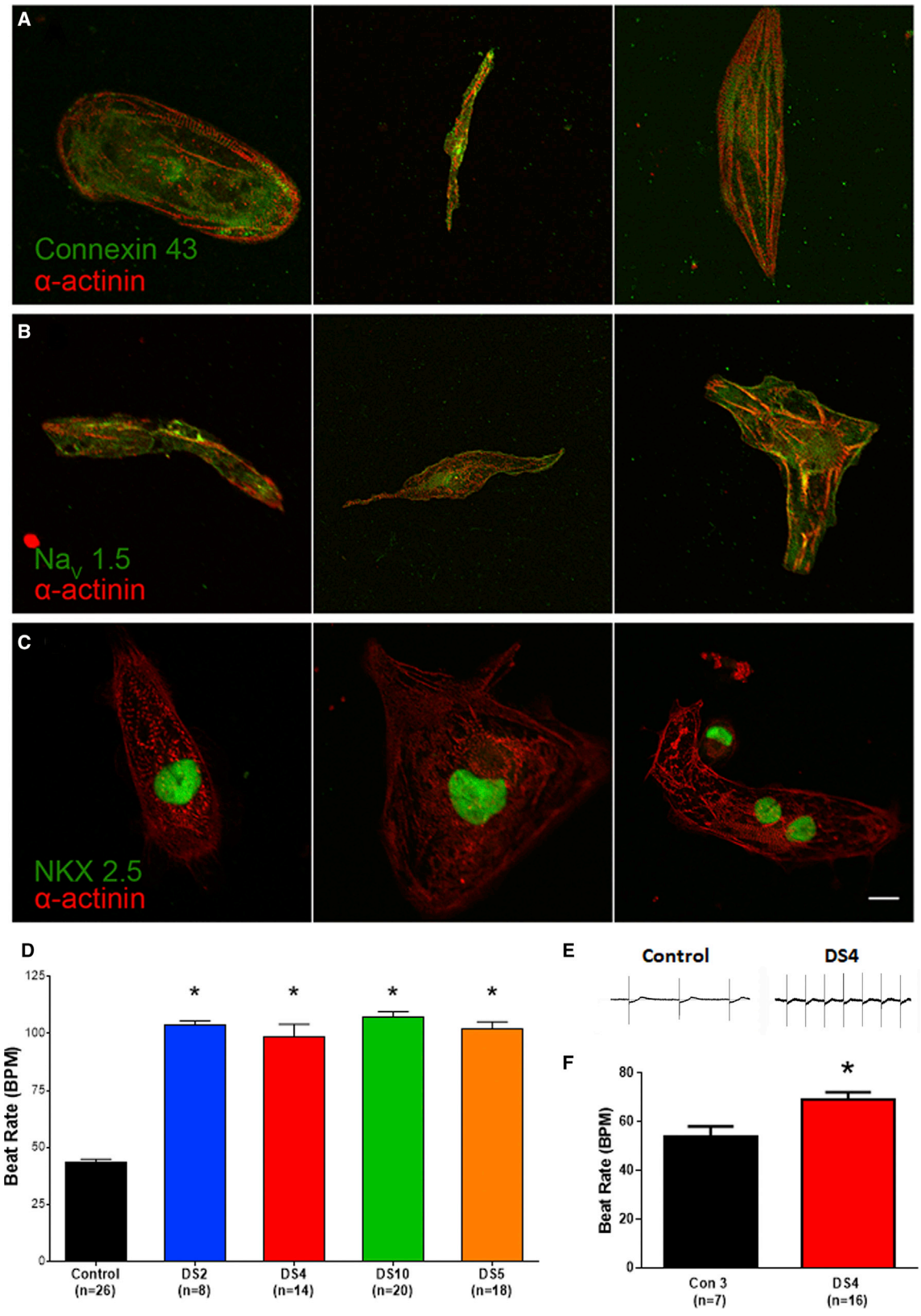

(legend on next page)

adult human heart. While there were measurable differences in *SCN5A* mRNA expression between the male and female control lines (1.9-fold increase in total *SCN5A* in female over male, 4.5-fold increase in *SCN5A-6* in female over male, and 3.7-fold increase in *SCN5A-6A* in female over male), there were no consistent differences in expression between the male and female DS lines, so the data for these lines were pooled. We observed increased total *SCN5A* expression in DS iPSC-CMs over the male control iPSC-CM line (3.2-fold) and over the female control line (1.7-fold), with adult human heart showing a 9.9-fold increase compared with the male control and a 5.2-fold increase compared with the female control. We also used specific primers to differentiate between adult (*SCN5A-6*) and embryonic (*SCN5A-6A*) splice variants of *SCN5A*. We observed a 4.6-fold increase in the combined DS iPSC-CM data over the male control but no difference compared with the female control. The DS iPSC-CM data also showed a 5.2-fold increase in the embryonic (*SCN5A-6A*) splice variant over the male control and a 1.5-fold increase over the female control. As expected, non-failing adult human heart had high levels of *SCN5A-6* with almost undetectable levels of *SCN5A-6A*.

Because our previous work in *Scn1b* null DS mice showed increased *Scn3a* mRNA, encoding the TTX-S VGSC $Na_v1.3$, and increased [^{3}H]saxitoxin binding, in addition to increased *Scn5a* and $Na_v1.5$ protein in the heart (Lin et al., 2015; Lopez-Santiago et al., 2007), we asked whether changes in TTX-S VGSC mRNA expression could account for the observed increase in I_{Na}. We found no differences in *SCN1A*, *SCN3A*, or *SCN8A* expression in the DS lines compared with controls (Figure S3A). Thus, our results suggest that, while compensatory upregulation of *SCN5A* in response to *SCN1A* haploinsufficiency partially contributed to the observed increases in I_{Na} in the DS lines, changes in TTX-S VGSC expression likely did not play a role.

As expected from previous reports (Doss et al., 2012; Herron et al., 2016), the level of *KCNJ2* mRNA (encoding $K_{ir}2.1$) expression was low in all iPSC-CM lines compared with the adult human heart samples (24.4-fold higher in non-failing adult human hearts compared with control iPSC-CM lines; Figure S3A), demonstrating a comparable level of maturity of all iPSC-CM lines tested. *NKX2.5*, a marker of cardiac development (Reecy et al., 1997), was present in all iPSC-CM lines as well as in human heart samples (Figures 1C and S3A).

To determine whether levels of *SCN5A* expression could be used as a potential biomarker for SUDEP, we performed qRT-PCR on autopsy samples obtained from two DS patients who died of SUDEP. When compared with non-failing adult human heart, there were no differences in total *SCN5A*, *SCN5A-6*, or *SCN5A-6A* expression (Figure S3B). We also investigated several common polymorphisms in *SCN5A* that are known to result in gain or loss of function, depending on the presence of other genetic mutations (Ackerman et al., 2004; Cheng et al., 2011; Hu et al., 2015; Kapplinger et al., 2015; Makielski et al., 2003; Shinlapawittayatorn et al., 2011; Ye et al., 2003). We tested the four most likely polymorphisms S524Y, H558R, 1077del, or R1193Q. However, none of the polymorphisms were present in either DS5 or control 2 (Figure S3C).

The large increase in I_{Na} density in DS5 iPSC-CMs compared with controls led to the recommendation that this patient receive a referral to a pediatric cardiologist for evaluation. Annual electrocardiography starting at 4 years of age revealed normal sinus rhythm without evidence of QT prolongation (corrected QT interval = 436 ± 5.4 ms, n = 3) but abnormal T-wave inversions and lateral T-wave flattening (Figure 3A and Table S2). A 2D echocardiogram showed normal ventricular size and function without significant intracardiac defects (data not shown). Because of the association of autonomic dysfunction in DS patients (Delogu et al., 2011), ambulatory 24-hr Holter monitoring was performed. Annual assessment demonstrated normal mean heart rates (Table S3) but very limited heart-rate variability with decreased time-domain parameters (root-mean-square of successive differences = 16.5 ± 1.1 ms and standard deviation of NN intervals = 57.9 ± 4.3 ms, n = 3) and altered frequency domain measurements (Figure 3B) (Jarrin et al., 2015).

Because patient DS5 exhibited T-wave abnormalities on the electrocardiogram, we recorded APs from control 2

Figure 1. Immunofluorescence Staining and Spontaneous Contraction Rates of iPSC-CMs

(A) Anti-α-actinin (red) and anti-connexin 43 (green) staining for DS5.

(B) Anti-α-actinin (red) and anti-Nav1.5 (green) staining for DS5.

(C) Anti-α-actinin (red) and anti-NKX 2.5 (green) staining for DS5.

(D) Increased contraction rates in DS iPSC-CM lines compared with control. Data from two independent control lines were pooled. For DS4, DS10, and DS5, data from two independent clones were pooled. For all lines, data were collected from 4–6 wells of one differentiation. *$p < 0.05$.

(E) Representative MEA traces from control (left) and DS (right) iPSC-CM lines.

(F) Quantification of contraction rates in MEA recordings. For control 3 (Con 3) and DS4, data were pooled from two different clones, with two independent differentiations per clone. *$p < 0.05$. Immunofluorescence staining of DS2, DS4, and DS10 is shown in Figure S1.

Data in (E) and (F) are presented as means ± SEM. Scale bar, 20 μm (A–C). See also Figure S2.

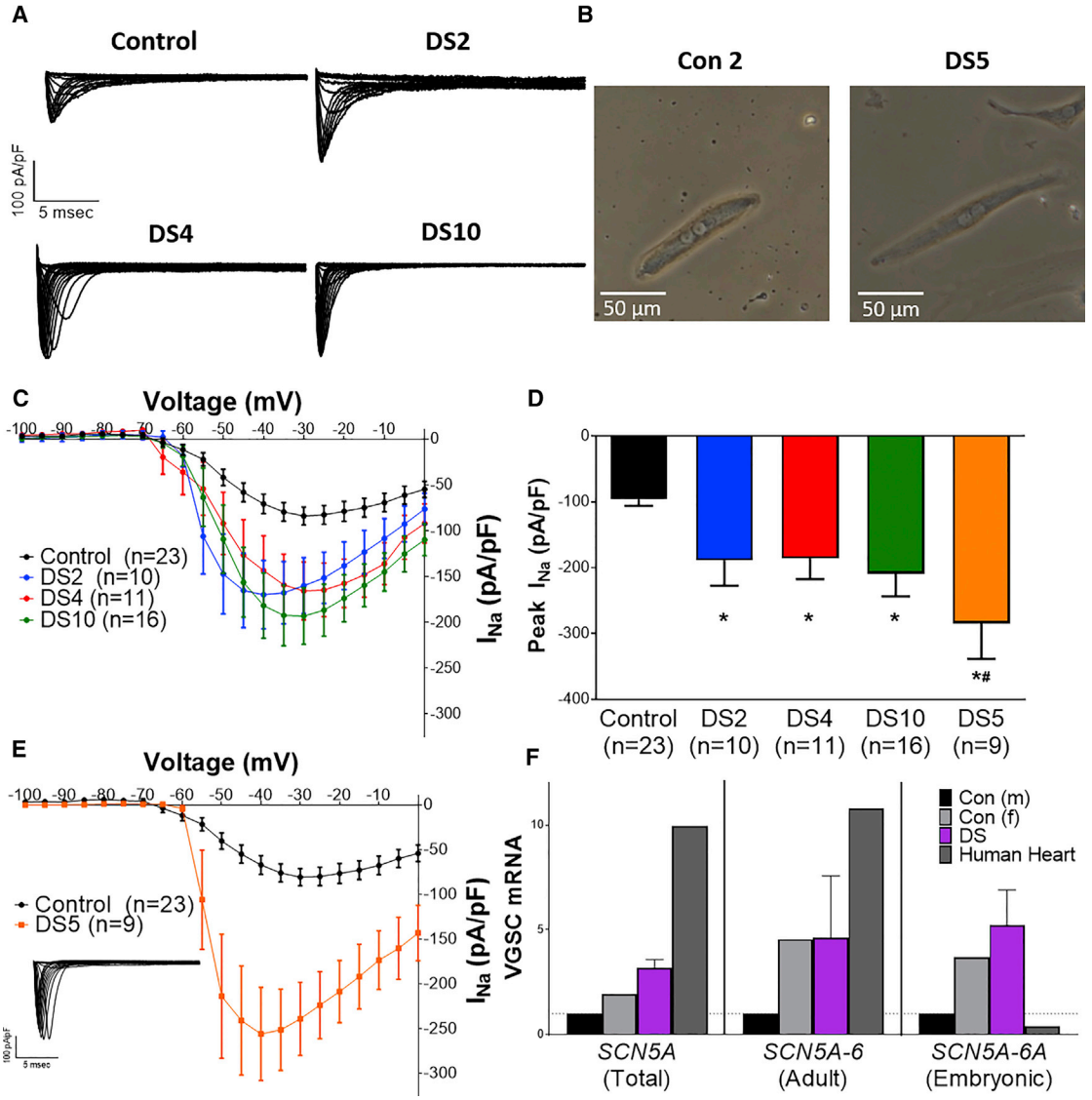

Figure 2. iPSC-CMs from DS Patients Have Increased Whole-Cell I_{Na} and Altered *SCN5A* Expression

(A) Representative whole-cell I_{Na} traces from a control and three DS subjects.

(B) Representative images of control 2 (Con 2) and DS5 iPSC-CMs used in electrophysiological recordings.

(C) I_{Na} current-voltage relationships for control and three DS iPSC-CM lines.

(D) Peak I_{Na} is increased in all four DS iPSC-CM lines compared with controls. *$p < 0.05$ versus control; #$p < 0.05$ versus average of DS2, DS4, and DS10.

(E) Current-voltage relationship comparing DS5 to control. Inset: representative I_{Na} trace from DS5. Peak I_{Na} data were pooled from two clones each for DS4, DS10, and DS5, respectively. Peak I_{Na} data for the control group were pooled from two independent control iPSC-CM lines (Con 2, 1 clone; Con 3, two clones). Data comparing the two control lines are shown in Figure S3. At least two independent differentiations were analyzed per line (Con 2, 3; Con 3-1, 2; Con 3-3, 2; DS2-3, 3; DS4-3, 3; DS4-4, 2; DS10-2, 4; DS10-7, 2; DS5-1, 2; DS5-2, 2).

(F) qRT-PCR data from male and female control iPSC-CM lines, pooled DS patient iPSC-CMs, and adult human heart control tissue.

Data in (C), (D), and (E) are presented as means ± SEM for all groups. For (F), data for DS samples are presented as means ± SEM (n = 4). See also Figures S3 and S4; Table S1.

and DS5 lines. We first treated iPSC-CMs with a viral construct to increase the expression of *KCNJ2* to generate a mature resting membrane potential, as described by Vaidyanathan et al. (2016). We found no differences in the resting membrane potential, threshold, AP duration (at 30%, 50%, 75%, or 90% repolarization), or amplitude

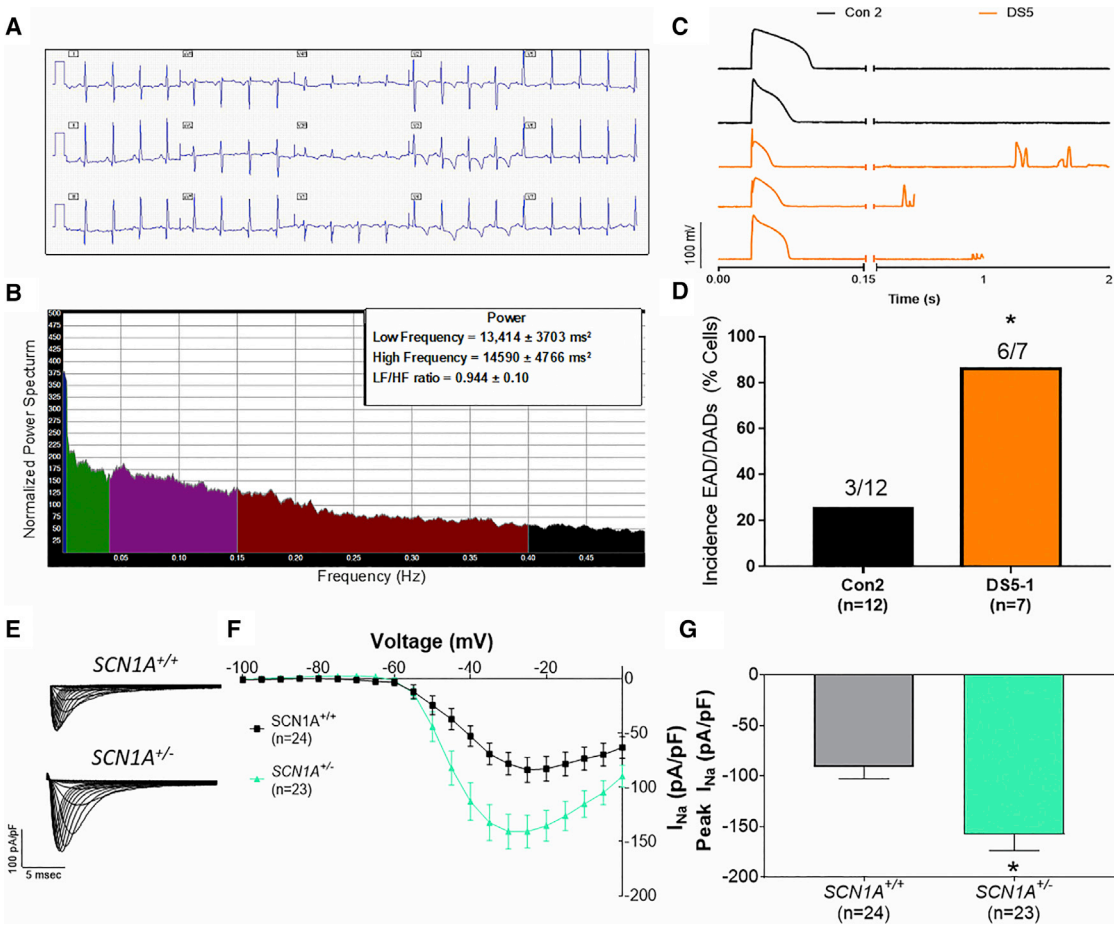

Figure 3. Abnormal Electrocardiogram and Limited Heart-Rate Variability in DS Subject 5, Arrhythmogenic Substrates in DS5 iPSC-CMs, and Increased Sodium Current Density in a CRISPR-Generated Heterozygous *SCN1A* Deletion Line

(A) Electrocardiogram recordings for DS subject 5 demonstrate normal sinus rhythm, T-wave inversions, and lateral T-wave flattening, abnormal for age.

(B) Representative power-spectrum analysis for heart-rate variability from 24-hr ambulatory Holter monitoring demonstrates limited short-term variability as compared with normal values for pediatric patients. Inset: compiled data from annual Holters, n = 3.

(C) Representative AP traces showing examples of delayed afterdepolarizations (DADs) in DS5 iPSC-CMs.

(D) Quantification of the incidence of early afterdepolarizations (EADs) and DADs in control and DS5 iPSC-CM lines. AP data for Con 2 and DS5 are from two independent differentiations each. *$p < 0.05$.

(E) Representative whole-cell I_{Na} traces from *SCN1A* heterozygous deletion (*SCN1A*$^{+/-}$) and isogenic control (*SCN1A*$^{+/+}$) iPSC-CMs.

(F) I_{Na} current-voltage relationships for *SCN1A*$^{+/-}$ and *SCN1A*$^{+/+}$ isogenic control iPSC-CM cells.

(G) Peak I_{Na} is increased in *SCN1A*$^{+/-}$ iPSC-CMs compared with the *SCN1A*$^{+/+}$ isogenic control line. Peak I_{Na} data for *SCN1A*$^{+/+}$ and *SCN1A*$^{+/-}$ are from two independent differentiations each. *$p < 0.05$ versus control.

Data in (F) and (G) are presented as means ± SEM. See also Figure S4; Tables S2 and S3.

between genotypes (Table S4). In contrast, there was an increase in the incidence of delayed afterdepolarizations (DADs) and early afterdepolarizations (EADs) in DS5 compared with the control (86% versus 25% of cells tested, respectively; $p = 0.02$; Figures 3C and 3D). DADs and EADs represent potential arrhythmogenic substrates that may exist at the whole-organ level. Their observed increased incidence in DS5 CMs is consistent with the electrocardiogram data as well as our previous observations in DS mouse models (Auerbach et al., 2013; Lin et al., 2015).

We used CRISPR gene editing (Tidball et al., 2017, 2018) to generate a heterozygous deletion in *SCN1A* (*SCN1A*$^{+/-}$) in a control line to ask whether Nav1.1 haploinsufficiency alone was sufficient to increase I_{Na} in iPSC-CMs, or whether this result was dependent on genetic background. The mutant clone used in this study had a heterozygous deletion of a cytosine at position 23

of the *SCN1A* cDNA (c.23del in NM_001165963.2), resulting in a mutation with a proline changed to a histidine at position 8, and a frameshift resulting in a premature stop codon at position 91 (p.P8HfsTer91) (Figure S4). The genotypes of the mutant and control lines were confirmed with next-generation sequencing of PCR amplicons of the targeted locus (Figure S4). The iPSC clones expressed the pluripotency markers SOX2, SSEA4, and OCT4 (Figure S4). Similar to the results in DS patient iPSC-CMs shown in Figure 2, we found a 1.75-fold increase in whole-cell I_{Na} density in the CRISPR *SCN1A*$^{+/-}$ iPSC-CMs compared with *SCN1A*$^{+/+}$ isogenic controls (Figures 3E–3G). In addition, CRISPR *SCN1A*$^{+/-}$ iPSC-CMS showed a small but significant negative shift in the voltage dependence of activation as well as a decrease in the slope of the inactivation curve compared with *SCN1A*$^{+/+}$ isogenic control (Table S5), consistent with the shift in the voltage dependence of activation observed in DS2 and DS10, as well as the decrease in slope observed in DS4 (Tables S1 and S5).

DISCUSSION

Taken together, our DS patient-derived iPSC-CM and limited clinical data suggest that the high risk of SUDEP in DS results from a predisposition to cardiac arrhythmias in addition to neuronal hyperexcitability, reflecting haploinsufficiency of *SCN1A* in heart and brain and the resulting compensatory overexpression of other VGSC genes in those tissues. We observed increased transient I_{Na} density and rates of spontaneous contraction in DS patient iPSC-CMs. For the subject with the most markedly increased I_{Na} density (patient DS5), increased incidence of arrhythmogenic AP substrates was recorded from iPSC-CMs, and cardiac and autonomic abnormalities were revealed upon clinical evaluation of the patient. This work demonstrates that iPSC-CMs are a valuable model for investigating SUDEP mechanisms in genetic ion-channel epilepsies and uncovering potential biomarkers of SUDEP risk.

EXPERIMENTAL PROCEDURES

Human Subjects

Fibroblast samples were obtained from human subjects under Institutional Review Board approval as described by Liu et al. (2013).

Statistics

Results are expressed as mean ± SEM. For contraction rate and electrophysiological recordings, a one-way ANOVA followed by Fisher's LSD post hoc test was used to compare iPSC-CM lines. Statistical significance was defined as $p < 0.05$.

Detailed methods for the generation of human iPSCs, CRISPR gene deletion, iPSC-CM differentiation and characterization, mRNA expression analyses, *SCN5A* sequencing, immunocytochemistry, MEA recording, and whole-cell voltage-clamp analysis are provided in Supplemental Information.

SUPPLEMENTAL INFORMATION

Supplemental Information includes Supplemental Experimental Procedures, four figures, five tables, and one video and can be found with this article online at https://doi.org/10.1016/j.stemcr.2018.07.012.

AUTHOR CONTRIBUTIONS

C.R.F. designed and performed the electrophysiology experiments, analyzed the data, sequenced *SCN5A*, and wrote the manuscript; H.Z. performed cardiac differentiations, measurements of contraction rates, and qRT-PCR analyses of iPSC-CMs; H.S. performed cardiac differentiations; J.O. performed immunofluorescence confocal analyses; L.T.D. generated the iPSC *SCN1A* CRISPR deletion in iPSCs; D.S.A. designed and performed preliminary electrophysiology experiments; V.J.B. performed and interpreted the clinical cardiac workup for patient DS5; C.C. assisted with DNA isolation and sequencing of *SCN5A*; A.G. provided postmortem cardiac mRNA samples from SUDEP patients; L.L.E. developed the *KCNJ2* viral construct; J.M.P. and L.L.I. designed and supervised the research and wrote the manuscript.

ACKNOWLEDGMENTS

This work was supported by NIH grants T32HL007853 and UL1TR000433 (fellowships to C.R.F.), R37-NS076752 (to L.L.I.), and U01-NS090364 (to J.M.P. and L.L.I.). Non-failing adult human heart surgical tissue samples were provided by Dr. Sharlene Day, University of Michigan.

Received: March 16, 2017
Revised: July 23, 2018
Accepted: July 26, 2018
Published: August 23, 2018

REFERENCES

Ackerman, M.J., Splawski, I., Makielski, J.C., Tester, D.J., Will, M.L., Timothy, K.W., Keating, M.T., Jones, G., Chadha, M., Burrow, C.R., et al. (2004). Spectrum and prevalence of cardiac sodium channel variants among black, white, Asian, and Hispanic individuals: implications for arrhythmogenic susceptibility and Brugada/long QT syndrome genetic testing. Heart Rhythm *1*, 600–607.

Auerbach, D.S., Jones, J., Clawson, B.C., Offord, J., Lenk, G.M., Ogiwara, I., Yamakawa, K., Meisler, M.H., Parent, J.M., and Isom, L.L. (2013). Altered cardiac electrophysiology and SUDEP in a model of Dravet syndrome. PLoS One *8*, e77843.

Bao, Y., and Isom, L.L. (2014). NaV1.5 and regulatory β subunits in cardiac sodium channelopathies. Card. Electrophysiol. Clin. *6*, 679–694.

Cheng, J., Tester, D.J., Tan, B.H., Valdivia, C.R., Kroboth, S., Ye, B., January, C.T., Ackerman, M.J., and Makielski, J.C. (2011). The

common African American polymorphism SCN5A-S1103Y interacts with mutation SCN5A-R680H to increase late Na current. Physiol. Genomics *43*, 461–466.

Claes, L., Del-Favero, J., Ceulemans, B., Lagae, L., Van Broeckhoven, C., and De Jonghe, P. (2001). De novo mutations in the sodium-channel gene SCN1A cause severe myoclonic epilepsy of infancy. Am. J. Hum. Genet. *68*, 1327–1332.

Cooper, M.S., McIntosh, A., Crompton, D.E., McMahon, J.M., Schneider, A., Farrell, K., Ganesan, V., Gill, D., Kivity, S., Lerman-Sagie, T., et al. (2016). Mortality in Dravet syndrome. Epilepsy Res. *128*, 43–47.

Delogu, A.B., Spinelli, A., Battaglia, D., Dravet, C., De Nisco, A., Saracino, A., Romagnoli, C., Lanza, G.A., and Crea, F. (2011). Electrical and autonomic cardiac function in patients with Dravet syndrome. Epilepsia *52* (*Suppl 2*), 55–58.

Doss, M.X., Di Diego, J.M., Goodrow, R.J., Wu, Y., Cordeiro, J.M., Nesterenko, V.V., Barajas-Martinez, H., Hu, D., Urrutia, J., Desai, M., et al. (2012). Maximum diastolic potential of human induced pluripotent stem cell-derived cardiomyocytes depends critically on I(Kr). PLoS One *7*, e40288.

Frasier, C.R., Wagnon, J.L., Bao, Y.O., McVeigh, L.G., Lopez-Santiago, L.F., Meisler, M.H., and Isom, L.L. (2016). Cardiac arrhythmia in a mouse model of sodium channel SCN8A epileptic encephalopathy. Proc. Natl. Acad. Sci. USA *113*, 12838–12843.

Herron, T.J., Rocha, A.M., Campbell, K.F., Ponce-Balbuena, D., Willis, B.C., Guerrero-Serna, G., Liu, Q., Klos, M., Musa, H., Zarzoso, M., et al. (2016). Extracellular matrix-mediated maturation of human pluripotent stem cell-derived cardiac monolayer structure and electrophysiological function. Circ. Arrhythm. Electrophysiol. *9*, e003638.

Hu, R.M., Tan, B.H., Tester, D.J., Song, C., He, Y., Dovat, S., Peterson, B.Z., Ackerman, M.J., and Makielski, J.C. (2015). Arrhythmogenic biophysical phenotype for SCN5A mutation S1787N depends upon splice variant background and intracellular acidosis. PLoS One *10*, e0124921.

Jarrin, D.C., McGrath, J.J., Poirier, P., Seguin, L., Tremblay, R.E., Montplaisir, J.Y., Paradis, G., and Seguin, J.R. (2015). Short-term heart rate variability in a population-based sample of 10-year-old children. Pediatr. Cardiol. *36*, 41–48.

Kalume, F., Westenbroek, R.E., Cheah, C.S., Yu, F.H., Oakley, J.C., Scheuer, T., and Catterall, W.A. (2013). Sudden unexpected death in a mouse model of Dravet syndrome. J. Clin. Invest. *123*, 1798–1808.

Kapplinger, J.D., Giudicessi, J.R., Ye, D., Tester, D.J., Callis, T.E., Valdivia, C.R., Makielski, J.C., Wilde, A.A., and Ackerman, M.J. (2015). Enhanced classification of Brugada syndrome-associated and long-QT syndrome-associated genetic variants in the SCN5A-encoded Na(v)1.5 cardiac sodium channel. Circ. Cardiovasc. Genet. *8*, 582–595.

Lian, X., Hsiao, C., Wilson, G., Zhu, K., Hazeltine, L.B., Azarin, S.M., Raval, K.K., Zhang, J., Kamp, T.J., and Palecek, S.P. (2012). Robust cardiomyocyte differentiation from human pluripotent stem cells via temporal modulation of canonical Wnt signaling. Proc. Natl. Acad. Sci. USA *109*, E1848–E1857.

Lin, X., O'Malley, H., Chen, C., Auerbach, D., Foster, M., Shekhar, A., Zhang, M., Coetzee, W., Jalife, J., Fishman, G.I., et al. (2015). Scn1b deletion leads to increased tetrodotoxin-sensitive sodium current, altered intracellular calcium homeostasis and arrhythmias in murine hearts. J. Physiol. *593*, 1389–1407.

Liu, Y., Lopez-Santiago, L.F., Yuan, Y., Jones, J.M., Zhang, H., O'Malley, H.A., Patino, G.A., O'Brien, J.E., Rusconi, R., Gupta, A., et al. (2013). Dravet syndrome patient-derived neurons suggest a novel epilepsy mechanism. Ann. Neurol. *74*, 128–139.

Lopez-Santiago, L.F., Meadows, L.S., Ernst, S.J., Chen, C., Malhotra, J.D., McEwen, D.P., Speelman, A., Noebels, J.L., Maier, S.K., Lopatin, A.N., et al. (2007). Sodium channel Scn1b null mice exhibit prolonged QT and RR intervals. J. Mol. Cell. Cardiol. *43*, 636–647.

Maier, S.K., Westenbroek, R.E., Schenkman, K.A., Feigl, E.O., Scheuer, T., and Catterall, W.A. (2002). An unexpected role for brain-type sodium channels in coupling of cell surface depolarization to contraction in the heart. Proc. Natl. Acad. Sci. USA *99*, 4073–4078.

Maier, S.K., Westenbroek, R.E., McCormick, K.A., Curtis, R., Scheuer, T., and Catterall, W.A. (2004). Distinct subcellular localization of different sodium channel alpha and beta subunits in single ventricular myocytes from mouse heart. Circulation *109*, 1421–1427.

Makielski, J.C., Ye, B., Valdivia, C.R., Pagel, M.D., Pu, J., Tester, D.J., and Ackerman, M.J. (2003). A ubiquitous splice variant and a common polymorphism affect heterologous expression of recombinant human SCN5A heart sodium channels. Circ. Res. *93*, 821–828.

Malhotra, J., Chen, C., Rivolta, I., Abriel, H., Malhotra, R., Mattei, L.N., Brosius, F.C., Kass, R.S., and Isom, L.L. (2001). Characterization of sodium channel alpha- and beta-subunits in rat and mouse cardiac myocytes. Circulation *103*, 1303–1310.

Meisler, M.H., and Kearney, J.A. (2005). Sodium channel mutations in epilepsy and other neurological disorders. J. Clin. Invest. *115*, 2010–2017.

Mishra, S., Reznikov, V., Maltsev, V.A., Undrovinas, N.A., Sabbah, H.N., and Undrovinas, A. (2015). Contribution of sodium channel neuronal isoform Nav1.1 to late sodium current in ventricular myocytes from failing hearts. J. Physiol. *593*, 1409–1427.

Radwanski, P.B., Brunello, L., Veeraraghavan, R., Ho, H.T., Lou, Q., Makara, M.A., Belevych, A.E., Anghelescu, M., Priori, S.G., Volpe, P., et al. (2015). Neuronal Na^+ channel blockade suppresses arrhythmogenic diastolic Ca^{2+} release. Cardiovasc. Res. *106*, 143–152.

Reecy, J.M., Yamada, M., Cummings, K., Sosic, D., Chen, C.Y., Eichele, G., Olson, E.N., and Schwartz, R.J. (1997). Chicken Nkx-2.8: a novel homeobox gene expressed in early heart progenitor cells and pharyngeal pouch-2 and -3 endoderm. Dev. Biol. *188*, 295–311.

Roden, D.M., Balser, J.R., George, A.L., Jr., and Anderson, M.E. (2002). Cardiac ion channels. Annu. Rev. Physiol. *64*, 431–475.

Shinlapawittayatorn, K., Du, X.X., Liu, H., Ficker, E., Kaufman, E.S., and Deschenes, I. (2011). A common SCN5A polymorphism modulates the biophysical defects of SCN5A mutations. Heart Rhythm *8*, 455–462.

Surges, R., Thijs, R.D., Tan, H.L., and Sander, J.W. (2009). Sudden unexpected death in epilepsy: risk factors and potential pathomechanisms. Nat. Rev. Neurol. *5*, 492–504.

Tidball, A.M., Dang, L.T., Glenn, T.W., Kilbane, E.G., Klarr, D.J., Margolis, J.L., Uhler, M.D., and Parent, J.M. (2017). Rapid generation of human genetic loss-of-function iPSC lines by simultaneous reprogramming and gene editing. Stem Cell Reports *9*, 725–731.

Tidball, A.M., Swaminathan, P., Dang, L.T., and Parent, J. (2018). Generating loss-of-function iPSC lines with combined CRISPR indel formation and reprogramming from human fibroblasts. Bio Protoc. *8*. https://doi.org/10.21769/BioProtoc.2794.

Vaidyanathan, R., Markandeya, Y.S., Kamp, T.J., Makielski, J.C., January, C.T., and Eckhardt, L.L. (2016). IK1-enhanced human-induced pluripotent stem cell-derived cardiomyocytes: an improved cardiomyocyte model to investigate inherited arrhythmia syndromes. Am. J. Physiol. Heart Circ. Physiol. *310*, H1611–H1621.

Veerman, C.C., Wilde, A.A., and Lodder, E.M. (2015). The cardiac sodium channel gene SCN5A and its gene product NaV1.5: role in physiology and pathophysiology. Gene *573*, 177–187.

Westenbroek, R.E., Bischoff, S., Fu, Y., Maier, S.K., Catterall, W.A., and Scheuer, T. (2013). Localization of sodium channel subtypes in mouse ventricular myocytes using quantitative immunocytochemistry. J. Mol. Cell. Cardiol. *64*, 69–78.

Westenbroek, R.E., Merrick, D.K., and Catterall, W.A. (1989). Differential subcellular localization of the R_I and R_{II} Na^+ channel subtypes in central neurons. Neuron *3*, 695–704.

Ye, B., Valdivia, C.R., Ackerman, M.J., and Makielski, J.C. (2003). A common human SCN5A polymorphism modifies expression of an arrhythmia causing mutation. Physiol. Genomics *12*, 187–193.

Yu, F.H., Mantegazza, M., Westenbroek, R.E., Robbins, C.A., Kalume, F., Burton, K.A., Spain, W.J., McKnight, G.S., Scheuer, T., and Catterall, W.A. (2006). Reduced sodium current in GABAergic interneurons in a mouse model of severe myoclonic epilepsy in infancy. Nat. Neurosci. *9*, 1142–1149.

Zhang, J., Wilson, G.F., Soerens, A.G., Koonce, C.H., Yu, J., Palecek, S.P., Thomson, J.A., and Kamp, T.J. (2009). Functional cardiomyocytes derived from human induced pluripotent stem cells. Circ. Res. *104*, e30–41.